PROCEEDINGS OF SCIENCE

The critical endpoint of the finite temperature phase transition for three flavor QCD with clover type fermions

Yoshifumi Nakamura[*†a], **Xiao-Yong Jin**[a], **Yoshinobu Kuramashi**[abc], **Shinji Takeda**[ad], **and Akira Ukawa**[c]

[a] *RIKEN Advanced Institute for Computational Science, Kobe, Hyogo 650-0047, Japan*

[b] *Graduate School of Pure and Applied Sciences, University of Tsukuba, Tsukuba, Ibaraki 305-8571, Japan*

[c] *Center for Computational Sciences, University of Tsukuba, Tsukuba, Ibaraki 305-8577, Japan*

[d] *Institute of Physics, Kanazawa University, Kanazawa 920-1192, Japan*

[†] *Email:* nakamura@riken.jp

We present preliminary results on the critical endpoint of three flavor QCD at zero chemical potential. We employ the renormalization-group improved Iwasaki gauge action and $O(a)$-improved Wilson fermion action. The critical endpoint is determined by using the intersection points of kurtosis for the temporal size N_t=4 and 6. We find the critical endpoint is around $m_{ud} = m_s \sim m_s^{phy}$ both at $N_t = 4$ and 6.

31st International Symposium on Lattice Field Theory LATTICE 2013
July 29 - August 3, 2013
Mainz, Germany

[*] Speaker.

PoS(LATTICE 2013)138

1. Introduction

Knowledge of the QCD phase structure is important in order to understand the physics of the early Universe, structure of neutron stars, processes in heavy-ion collisions experiments, etc. To study the QCD phase transition, non-perturbative treatment is necessary. Lattice QCD is the most suitable way to solve QCD non-perturbatively. There is, however, sign problem at simulations with finite chemical potential. Thus, it is important to understand the lower left corner of the Columbia phase diagram plot at zero density which depicts the nature of the finite temperature phase transition as a function of light u-d quark masses and strange quark mass before starting extensive studies at finite chemical potential.

The results of previous studies for the region of first order phase transition at zero chemical potential are very contradict between staggered type and Wilson type fermions. All results with staggered type fermions using the rooting of quark determinant and with different levels of improvement are consistent with the physical point being in the crossover region [1, 2, 3, 4]. In contrast, results with Wilson type fermions which used the simple Wilson action found that the physical point exist in the first order phase transition region [5]. To clarify the issue, an independent investigation which contains results taken to the continuum limit is needed.

2. Methods

In this work we perform simulations with Iwasaki gauge action [6] and $N_f = 3$ dynamical flavors of non-perturbatively $O(a)$-improved Wilson fermion action [7] on lattices of temporal extent $N_t = 4, 6$ and determine the critical endpoint on the line of $m_s = m_{ud}$, *i.e.*, we perform simulations with mass-degenerate sea quarks for all 3 flavors. Wilson type fermions have exact flavor symmetry, which we consider to be a big advantage over staggered fermions, as the finite temperature phase transition largely depends on the flavor degrees of freedom. A disadvantage though is lack of chiral symmetry.

We generate O(10,000 – 200,000) trajectories for each ensemble. At $N_t = 4$, we choose spatial lattice size $N_l = 6, 8, 10$ and cover the range $\kappa = 0.143 - 0.144$ at $\beta = 1.60$, $\kappa = 0.1405$–0.142 at $\beta = 1.65$, $\kappa = 0.1375$–0.1395 at $\beta = 1.70$. At $N_t = 6$, we choose $N_l = 10, 12, 16$ and cover the range $\kappa = 0.1403 - 0.1405$ at $\beta = 1.73$, $\kappa = 0.1395$–0.1398 at $\beta = 1.75$, $\kappa = 0.1385$–0.1392 at $\beta = 1.77$.

We compute plaquette, P, gauge action density, s_g, Polyakov loop, L, their susceptibility, χ , skewness, S , and kurtosis, K, defined respectively by

$$P = \frac{1}{6N_l^3 N_t} \sum_{\mu<\nu} \frac{1}{3} \mathrm{ReTr}\, W_{\mu\nu}^{1\times 1}, \tag{2.1}$$

$$s_g = c_0(1-P) + 2c_1(1-R), \quad R = \frac{1}{12N_l^3 N_t} \sum_{\mu\neq\nu} \frac{1}{3} \mathrm{ReTr}\, W_{\mu\nu}^{1\times 2}, \tag{2.2}$$

$$L = \frac{1}{N_l^3} \sum_{\vec{x}} L(\vec{x}), \quad L(\vec{x}) = \frac{1}{3} \mathrm{Tr} \prod_{x_4=1}^{N_t} U_4(x), \tag{2.3}$$

$$\chi = V\langle (O - \langle O\rangle)^2 \rangle, \quad S = \frac{\langle (O-\langle O\rangle)^3\rangle}{\langle (O-\langle O\rangle)^2\rangle^{3/2}}, \quad K = \frac{\langle (O-\langle O\rangle)^4\rangle - 3(\langle (O-\langle O\rangle)^2\rangle)^2}{\langle (O-\langle O\rangle)^2\rangle^2}, \tag{2.4}$$

where $W_{\mu\nu}^{i\times j}$ is $i\times j$ Wilson loop, $c_0 = 1-8c_1$, $c_1 = -0.331$ and O is an observable. Kurtosis K can be written using Binder cumulant as,

$$K = B_4 - 3, \quad B_4(O) = \frac{\langle (O-\langle O\rangle)^4\rangle}{\langle (O-\langle O\rangle)^2\rangle}, \tag{2.5}$$

which is frequently used to determine the critical point. These quantities are often better than the maximum point of susceptibility because finite size effects is much smaller. For example, magnetization in the Ising model behaves like

$$M = N_l^{-\beta'/\nu} f_M(tN_l^{1/\nu'}) \tag{2.6}$$

with reduced temperature, t, and critical exponents, β' and ν' in finite size systems. By using this scaling function, $B_4(M)$ can be written as

$$B_4(M) = \frac{N_l^{-4\beta'/\nu} f_{M^4}(tN_l^{1/\nu'})}{[N_l^{-2\beta'/\nu} f_{M^2}(tN_l^{1/\nu'})]^2} = f_B(tN_l^{1/\nu'}). \tag{2.7}$$

Therefore K does not depend on volume at a second order phase transition point. At the first order phase transition point, for large volumes, K reaches the minimum [8] according to

$$K = -2 + \frac{c}{N_l^d} + O(1/N_l^{2d}). \tag{2.8}$$

In the case of crossover, there is no such formula. But we can expect that the distribution becomes sharper, and K becomes larger, with increasing volume.

We use this property of K to determine the critical endpoint. So our strategy is as follows.

- First we find the transition point by using a fit around the peak of susceptibilities at each N_l.
- Then we obtain K at the transition point, $K_{\rm t}$, at each N_l.
- Finally we find the intersection point of $K_{\rm t}$ by fit with finite size scaling inspired ansatz [2]

$$f(\beta, N_l) = K_{\rm E} + aN_l^{1/\nu}(\beta-\beta_{\rm E}) + bN_l^{2/\nu}(\beta-\beta_{\rm E})^2, \tag{2.9}$$

where $K_{\rm E}$, $\beta_{\rm E}$ and ν are the kurtosis, β at the critical endpoint, and the critical exponent, respectively. It is expected that the critical endpoint of $N_f = 3$ (also $N_f = 2+1$) QCD belongs the universality class of the 3D Ising model [9]. Therefore $K_{\rm E} = -1.396$ and $\nu = 0.63$ are the expected values. However, we do not assume any value for $K_{\rm E}$ and ν in this study. We also compute pseudoscalar and vector meson mass ratio at the transition point, $(m_{PS}/m_V)_{\rm t}$ to obtain the ratio at the critical endpoint, $(m_{PS}/m_V)_{\rm E}$, by interpolation.

3. Results

The range of β in this study is rather low as compared to usual zero temperature simulations. So we first check that we are looking at real finite-temperature phase transition, and not a bulk (lattice artifact) phase transition since κ in our simulation is slightly larger than the region confirmed to be absent of the bulk phase transition in ref. [10] ($\kappa \lesssim 0.14$). In Fig. 1 we plot P both on $6^3\times 4$ and

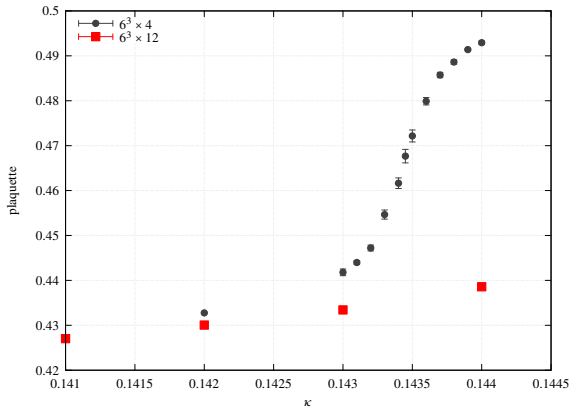

Figure 1: P v.s. κ both on $6^3 \times 4$ and $6^3 \times 12$ at $\beta = 1.60$.

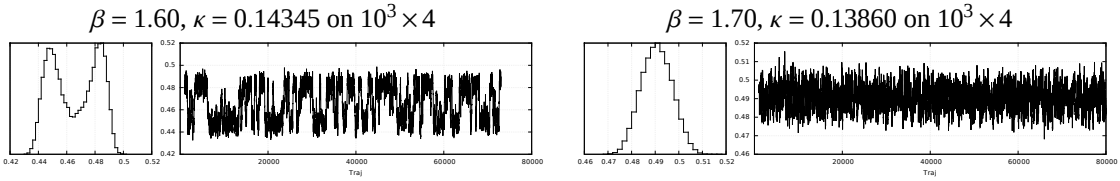

Figure 2: Representative case for history and histogram at first order phase transition point (left). Representative case for history and histogram at crossover (right).

$6^3 \times 12$ at $\beta = 1.60$. We see there is finite temperature phase transition at $\kappa \sim 0.1435$, and no bulk phase transition at zero temperature simulation in this region.

Figure 2 shows representative cases for time history and histogram at first order phase transition point and crossover point. We see a clear double peak distribution and a two state signal of low and hight temperature phases for the case of first order phase transition. On the other hand, there is no such behavior for the crossover case [1].

In Figs. 3–5 we present results for expectation value, susceptibility, skewness and kurtosis for P and L, together with quadratic fitting results for susceptibility and kurtosis at $N_t = 4$. We find that the maximum location of χ, the point where S is zero near the transition point and the minimum location of K are almost on the same point. At $\beta = 1.60$, a dip of K becomes sharper and deeper for larger volumes. We observe that the minimum of K becomes larger with increasing volume at $\beta = 1.65, 1.70$.

In Fig. 6 we plot K_t with fitting results of eq. (2.9) and $(m_{PS}/m_V)_{\rm t}$ with linear fitting results. To obtain $\beta_{\rm E}$, since we have three observables, we minimize the following χ^2

$$\chi^2 = \sum_{O=P,L,s_g} \left[\frac{K_O(\beta, N_l) - f_O(\beta, N_l)}{\delta K_O(\beta, N_l)} \right]^2, \tag{3.1}$$

where $\delta K_O(\beta, N_l)$ is the error of $K_O(\beta, N_l)$. We obtain $\beta_{\rm E} = 1.6274(30)$ at $N_t = 4$ and $\beta_{\rm E} = 1.7345(12)$ at $N_t = 6$. For $(m_{PS}/m_V)_{\rm E}$, we fit data with linear function and obtain 0.7289(28) and 0.6653(20)

[1] To distinguish first order, second order and or crossover transition, one must compare kurtosis at different volumes.

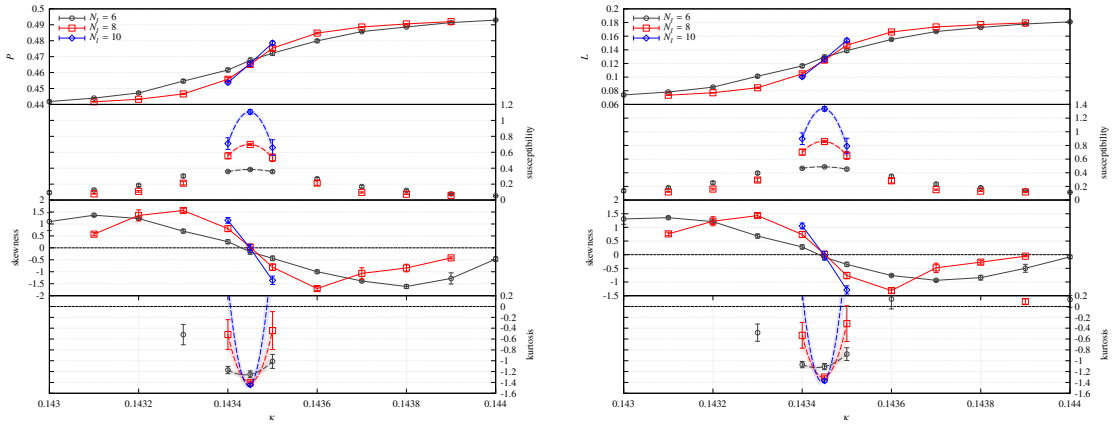

Figure 3: Expectation value, susceptibility, skewness and kurtosis (from top to bottom in panel) for plaquette (left) and Polyakov loop (right) at $\beta = 1.60$ and $N_t = 4$, together with quadratic fit for susceptibility and kurtosis.

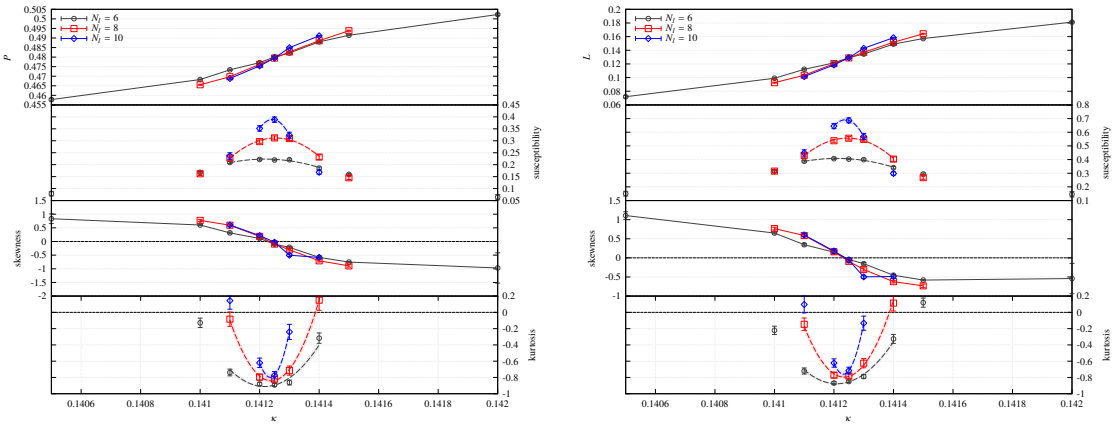

Figure 4: Same as Fig. 3, but at $\beta = 1.65$.

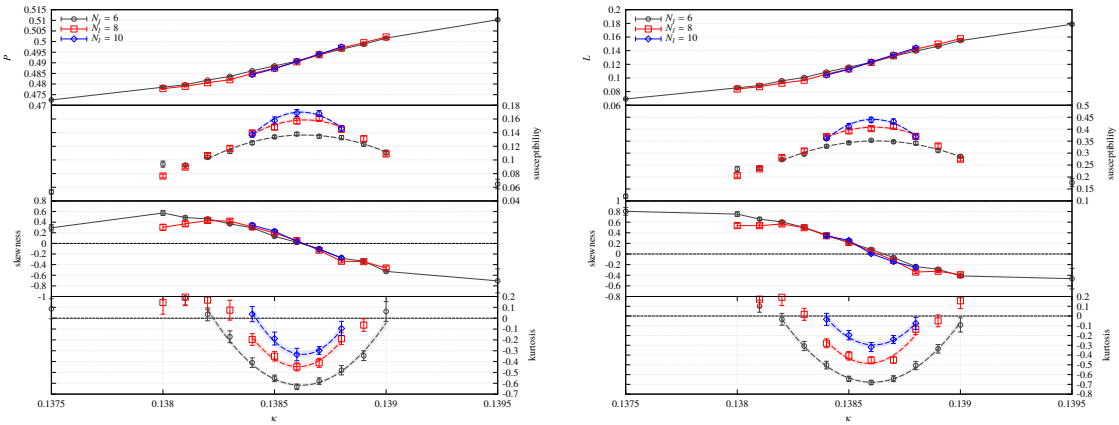

Figure 5: Same as Fig. 3, but at $\beta = 1.70$.

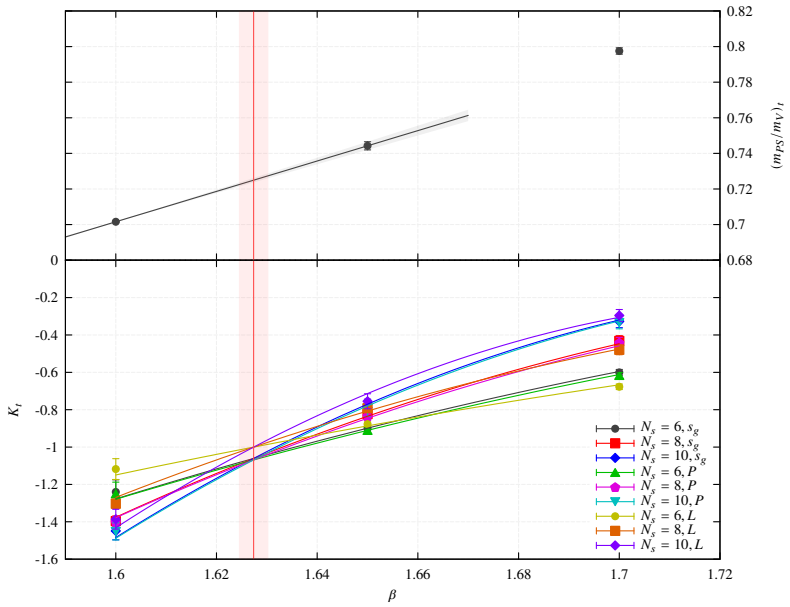

Figure 6: $K_{\rm t}$ v.s. β with fitting results of eq. (2.9) at $N_t = 4$

at $N_t = 4$ and 6, respectively. In Fig. 7 we plot $(m_{PS}/m_V)_{\rm E}$ as a function of $1/N_t^2$. The black points indicate (m_{PS}/m_V) at the critical endpoint for each N_t. The blue diamond point indicates the flavor SU(3) symmetric point defined by $m_q = (m_u^{phy} + m_d^{phy} + m_s^{phy})/3$. The green triangle indicates the point where all three quark masses are equal to the physical strange quark mass. We find that the transition is first order for $(m_{PS}/m_V) \lesssim 0.7$, is a crossover for $(m_{PS}/m_V) \gtrsim 0.7$ at $N_t = 4, 6$. We also observe that $(m_{PS}/m_V)_{\rm E}$ becomes smaller with increasing N_t. Since there are only two points, we need further investigation at larger N_t to extrapolate to the continuum limit.

4. Summary

We have investigated the critical endpoint of QCD at $\mu = 0$ with $N_f = 3$ degenerate dynamical flavors of non-perturbatively $O(a)$-improved Wilson fermions. We have determined the critical endpoint by using the intersection points of kurtosis at $N_t = 4, 6$. We have found for these temporal lattice sizes that, along the flavor symmetric line with $m_s = m_{ud}$, the critical end point is located around the point where all three quark masses are equal to the physical strange quark mass. We are extending our study to larger N_t to obtain conclusive results in the continuum limit.

Acknowledgments

This research used computational resources of the K computer provided by the RIKEN Advanced Institute for Computational Science (AICS) through the HPCI System Research project (Project ID:hp120115), GPU cluster at RIKEN AICS, FX10 at University Tokyo and Kyushu University. The BQCD code [11] was used in this work.

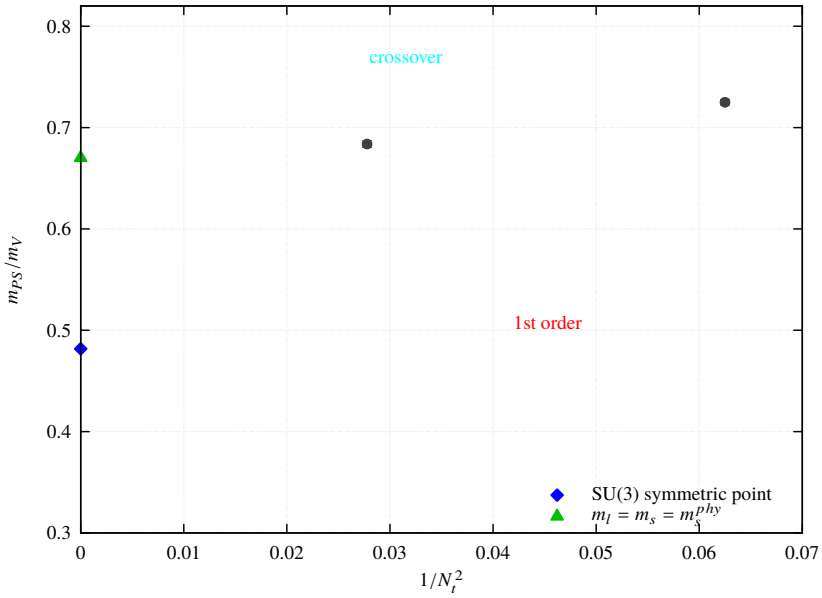

Figure 7: $(m_{PS}/m_V)_{\rm E}$ v.s. $1/N_t^2$. ◆ denotes the flavor SU(3) symmetric point, $m_{PS}^{phy;sym}/m_V^{phy;sym} = \sqrt{(m_\pi^2+2m_K^2)/3}/[(m_\rho+2m_{K^*})/3] \sim 0.4817$. ▲ denotes $m_{ud} = m_s = m_s^{phy}$, $m_{\eta_{ss}}/m_\phi \sim 0.6719$.

References

[1] F. Karsch, E. Laermann and C. Schmidt, Phys. Lett. B **520** 41 (2001), [arXiv:hep-lat/0107020].

[2] P. de Forcrand and O. Philipsen, JHEP **0701**:077 (2007), [arXiv:hep-lat/0607017].

[3] G. Endrődi, *et. al.*, PoS, **LAT2007** 182 (2007), [arXiv:0710.0998 [hep-lat]].

[4] H.-T. Ding, *et. al.*, PoS, **LAT2011** 191 (2011), [arXiv:1111.0185 [hep-lat]].

[5] Y. Iwasaki, *et. al.*, Phys.Rev. D **54** 7010 (1996), [arXiv:hep-lat/9605030].

[6] Y. Iwasaki, Report No. UTHEP-118, 1983 (unpublished), [arXiv.1111.7054].

[7] S. Aoki, *et al.* (CP-PACS and JLQCD Collaborations), Phys. Rev. D **73**, 034501 (2006).

[8] A. Billoire, *et al.*, Nucl. Phys. **B370**, 773 (1992).

[9] S. Gavin, *et al.*, Phys. Rev. D **49** 3079 (1994).

[10] S. Aoki *et al.* (JLQCD Collaborations), Phys. Rev. D **72** 054510 (2005), [arXiv:hep-lat/0409016].

[11] Y. Nakamura and H. Stüben, PoS **LATTICE2010** 040 (2010), [arXiv:1011.0199 [hep-lat]].